

Analysis of the Behaviour of Composite Connections in Multi-Storey Buildings Under Earthquake Loading

Milijaš, Aleksa

Abstract: *In the past years, number of beams and slabs in steel structures that are executed as composite steel – concrete elements has significantly increased. In moment-resisting frames with composite steel – concrete slabs, slab reinforcement in tensile zone needs to be considered in design of composite steel – concrete beam – to – column connections with steel plates and bolts in tensile zone. However, the number of reinforcement bars that should be taken into account in connection design significantly depends on the effective width of the concrete slab. Moreover, directions for calculation of the effective width of the concrete slab are still not unambiguous as they can be calculated either according to recommendations from Eurocode 4 or Eurocode 8. In this paper, composite connections are briefly explained and main differences between composite steel – concrete beam – to – column connections and corresponding steel connections are summarized. Furthermore, behaviour of a composite steel – concrete beam – to – column connection under bending moment and shear force induced by earthquake loading is investigated using finite element analysis in software package Abaqus. Finally, a parametric study is carried out in order to examine the suitability of two code recommendations for determination of the effective width of concrete slab in case of seismic loading.*

Index Terms: *Composite, connection, moment-resisting, width, slab, earthquake*

1. INTRODUCTION

BEAM-COLUMN connections in usual steel moment – resisting frames are executed with steel plates and bolts. Under seismic loading these connections may be loaded with positive and negative bending moments and shear forces. In case of negative bending moments, upper row of bolts is subjected to tensile forces. The transfer of forces in a usual steel beam – to – column connection is shown in Figure 1. Furthermore, in case of constructions with composite steel – concrete slabs, slab reinforcement located in the

beam – column joint area is also subjected to tensile forces under negative moments. The activation of this reinforcement leads to increase of moment capacity and rotational stiffness of composite steel – concrete beam – to – column connections. The force transfer in a composite steel – concrete beam – to – column connection is presented in Figure 2. By varying some parameters of the composite slab, such as the width and thickness of concrete slab or amount of reinforcement or degree of coupling, it is possible to construct the composite connection with desired characteristics. However, the design of composite connection needs to be done in accordance with available simple code directions.

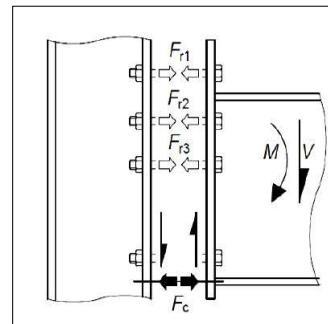


Figure 1. Force transfer in regular steel beam – to – column connection

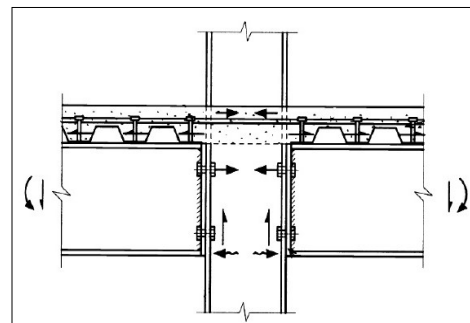


Figure 2. Force transfer in composite steel – concrete beam – to – column connection

2. PROBLEM STATEMENT

For design of steel – concrete beam – to – column composite connections, the component

approach accepted by Eurocode 4 [1] is currently in use. This approach is used for calculation of moment capacity of typical steel constructions too, as it is shown in Figure 3. However, for composite joints, presence of slab reinforcement in tensile zone is considered too (Figure 4). In Table 1 components of composite connection subjected to negative bending moment and shear force are summarized.

ZONE	INDEX	COMPONENT
TENSION	a	bolts in tension
	b	steel plate under bending
	c	column flange under bending
	d	beam web in tension
	e	column web under transverse tension
	f	welds
	g	welds
	r	longitudinal reinforcement in tension
SHEAR	h	column web under shear
COMPRESSION	j	beam flange and web under compression
	l	column web under compression

Table 1. Components of composite connection

The amount of longitudinal reinforcement in composite connection (component r) is directly dependent on the effective width of concrete slab. Therefore, the variation of the effective width of concrete slab has a significant influence on the tensile force that is transferred by longitudinal reinforcement and on the overall moment capacity of the composite connection.

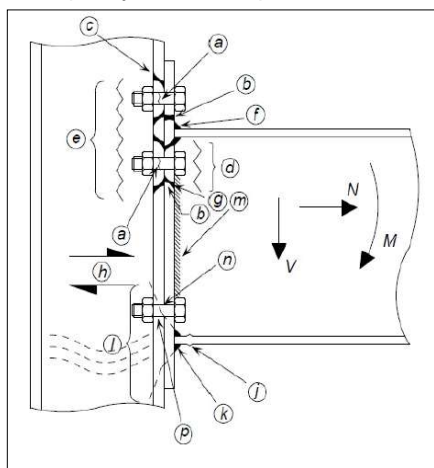


Figure 3. Components of steel moment connection

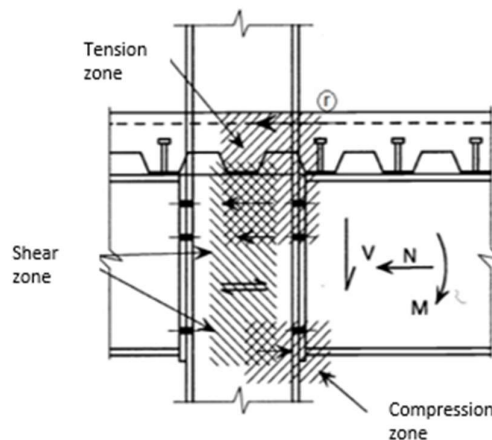


Figure 4. Additional component for composite moment connection

3. THE BEST EXISTING SOLUTIONS

As the whole design of composite connections is carried out according to Eurocode 4 [1], the effective slab width (b_{eff}) can be determined following the recommendations provided by Eurocode 4 [1]. However, for case of seismic combination, which is usually relevant in multi-storey buildings, Eurocode 8 [2] also offers recommendations for determination of effective slab width (b_{eff}). Depending on different parameters of considered composite connections, adoption of different effective slab widths may result in different connection capacities. Therefore, this topic desires further investigation.

4. THE PROPOSED SOLUTION

In this paper, effects of the variation of the effective slab width will be studied in detail on an example of a typical composite connection and recommendation for design in practice will be provided.

The considered steel – concrete composite connection is shown in Figure 5. It is a beam – to – column connection in a moment-resisting frame of a regular 9-story commercial building. For beams, IPE360 steel profile is used which is covered by a profiled steel sheet (CF60) and concrete slab. Diameter of reinforcement bars is 12 mm and distance between them is 100 mm. Composite action is provided by connecting steel profiles with covering concrete slab by shear stud connectors that have 25 mm diameter and are welded to the steel IPE 360 profile at every 100 mm. Column is a steel HEB 500 profile. Connection between beam and column is executed by a steel plate and bolts. Since it is a composite connection, longitudinal reinforcement in concrete slab is considered too. More detailed description of the rest of the building and its

design that has been carried out in accordance with Eurocode 1 [3], Eurocode 3 [4], Eurocode 4 [1] and Eurocode 8 [2] can be found in [5].

In order to further investigate the behaviour of the structure under seismic loading, linear time-history analysis was carried out. Accelerograms of earthquakes Vrancea (1997), Petrovac (1979), Banja Luka (1969) and Mionica (1998) were first scaled against the value of the reference maximum ground acceleration, which is around 0.12g for Belgrade. This scaling was done as the focus of the investigation is the behaviour of the structure under the design loads. Afterwards, the scaled accelerograms which correspond to design loads were assigned as a horizontal load to the spatial model in software package SAP2000 [6]. The bending moments and shear forces in the considered joint were recorded. Since the highest values of bending moments and shear forces were recorded for the scaled accelerogram of earthquake Vrancea (1997), the behaviour of composite steel – concrete connection is studied under these forces using finite element analysis in a software package Abaqus [7].

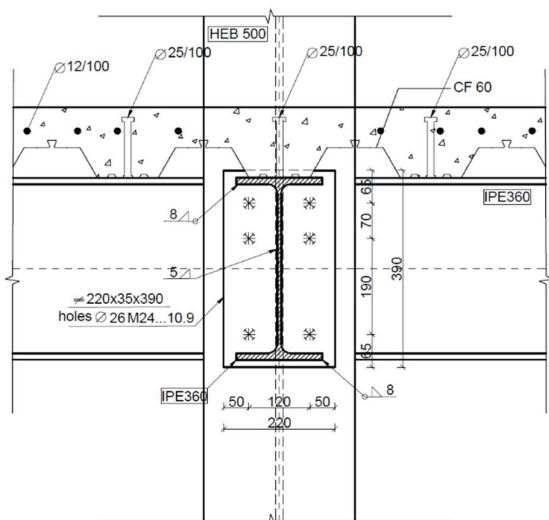


Figure 5. Beam – to – column connection

5. CONDITIONS OF THE ANALYSIS TO FOLLOW

For detailed investigation of performance of considered composite connection designed according to Eurocode 4 [1] and Eurocode 8 [2] under seismic loading, a 3D numerical model built in software package Abaqus [7] is used. Since the selected connection transfers the forces in only one direction, elements that transfer forces in the perpendicular direction have been neglected in the model. In the analysis, stresses and strains in all connection elements are analyzed, as well as level of plastification. In a parametric study, three effective widths of concrete slab are investigated under seismically

induced bending moment and shear force.

6. DETAILS OF THE PROPOSED SOLUTION

Composite connection shown in Figure 5 has been analyzed by means of a finite element method. In the following, details of the numerical model used in the study will be presented.

6.1 Numerical model – Geometry and boundary conditions

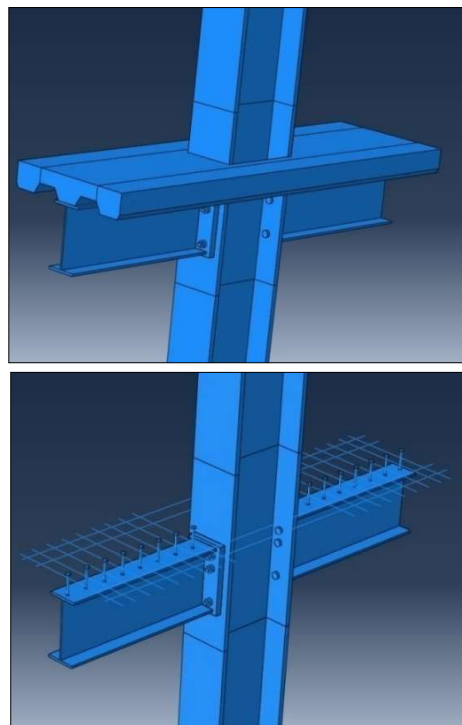


Figure 6. Model of composite connection in Abaqus [7]

The model is built of a steel column and beam, steel plate, bolts, shear stud connectors and concrete plate with reinforcement (Figure 6). Steel elements are modelled as 3D (solid) elements. The simple *tie constraint* is used to represent the welded connection between steel beam profile and steel plate. Furthermore, body and head of shear stud connectors are modelled as one element (part) and connection between shear stud connectors and steel beams is realized as *tie constraint*. Body and head of one bolt are modelled as one element (part). For the sake of simplicity, thread is not modelled and nut and bolt thus make a *tie constraint* connection. 3D solid elements are also used to model concrete slab. The bottom edge of a concrete slab corresponds to the shape of the trapezoidal steel sheet profile. The width of concrete slab is equal to corresponding effective width in considered section, whereas the length of concrete slab corresponds to the length of beams used in model. Reinforcement bars are modelled as wire 3D-Truss (T3D2) elements. Interaction

between concrete and reinforcement is provided by option *Constraint – Embedded* region. Column length corresponds to the two floor heights, where the analyzed joint is located in the middle. Simple boundary conditions are applied - all displacements and rotations of nodes at the edge surfaces of columns are restrained.

6.2 Numerical model – Loading

The analysis is divided into two steps. In the first step (*Initial step*) boundary conditions and all interactions between elements in this composite connection are defined. Option *General Contact* is used to define global interaction between all elements that are in contact. In the scope of *General Contact*, options *Tangential* and *Normal behaviour* are defined. By the first option friction between two elements that are in contact is defined by setting friction coefficient to 0.25 and definition of normal behaviour prevents elements penetrating each other under applied loads. In the second step (*Loading step*) maximum bending moment and maximum shear force extracted from the linear time-history analysis of a 3D building model in SAP 2000 [6] are applied to the beam element in a finite element model in Abaqus [7] (Figure 7). Uniform application of load is achieved by using the option *Constraint – Coupling*. The center of gravity of uncracked composite section is used as a reference point to which the load is applied. This point is connected with the surface of composite section by *Constraint-coupling* option. *Smooth-step* is used as an amplitude type for all loads to ensure smooth load application.

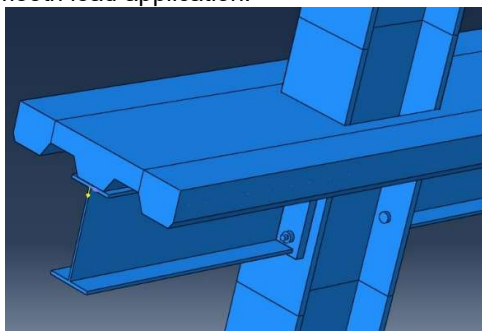


Figure 7. Model with applied load

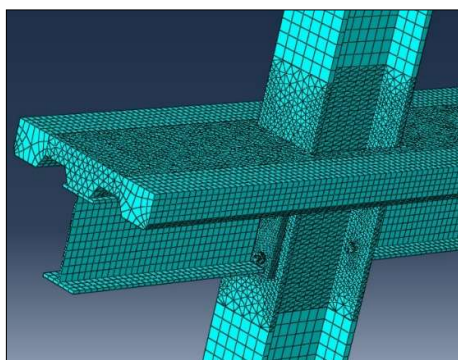


Figure 8. Model with generated mesh

6.3 Numerical model – Finite element mesh

In this study, the *Explicit Dynamic Analysis* is applied. According to recommendations from Abaqus [7], for this analysis type, C3D8R finite elements (*hexahedral continuum 8-node finite elements with reduced integration*) are adopted as the most appropriate. However, on parts of the column that have holes for bolts, as well as in parts of concrete slab close to the shear stud connectors, C3D4 finite elements (*tetrahedral finite elements*) are used. Application of these finite elements provides better approximation of circular and curved model geometry. T3D2 finite elements are used for reinforcement bars, as they correspond to the selected element and cross section that are used to model reinforcement bars.

The smallest mesh size is used for bolts and nuts (3 mm), while mesh used for shear stud connectors is slightly coarser (4 mm). For modelling of steel plates mesh size is 10 mm, while for steel beams and concrete slab it is 30 mm. Reinforcement bars are modelled by 10 mm long finite elements. Mesh on the column parts around holes for bolts is denser (20 mm) than on column parts closer to restraints (50 mm).

6.4 Numerical model – Materials

Columns, beams and steel plates are made of steel S355. Strength class of M24 bolts is 10.9. In model, elastic and plastic behaviour is taken into account for all steel elements. The true stress-strain diagrams are used as an input data and they are extracted from the nominal stress-strain diagrams obtained in experimental tests.

The true stress-strain diagrams are also used to model B400/500 steel reinforcement. They are also obtained from the nominal stress-strain diagrams obtained from experimental tests.

For concrete modelling *Concrete Damaged Plasticity (CDP)* model available in Abaqus [7] is used. This model allows definition of material behaviour depending on the stress type. Namely, stress-strain relationships are separately defined for the case of compressive and tensile stresses. Used plasticity parameters presented in Table 2 are adopted according to recommendations available in the literature [8-11].

Dilation Angle	Eccentricity	f_{b0}/f_{c0}	K	Viscosity Parameter
36	0.1	1.2	0.59	0

Table 2. Plasticity parameters for CDP model

Parameters that define material behaviour in elastic range are adopted according to Table 3.1 from Eurocode 2 [12]. Therefore, elasticity modulus for the used strength class is $E_{cm} = 33$ GPa and Poisson's ratio is $\nu = 0.2$. Strain that corresponds to stress of $0.4f_{cm}$ ($f_{cm} = 38$ MPa) is set as elasticity limit. Plastic part of stress-strain curve is defined separately in compression and

tension. Stress-strain relation in compression in plastic range is composed of several segments (Figure 9). Stress equal to $0.4f_{cm}$ and corresponding strain are considered as onset of plastic range. Stress values that correspond to strains between ε_{el} и ε_{cu1} are defined by equations proposed in Eurocode 2 [12]:

$$\sigma_c = f_{cm} \cdot \frac{k\eta - \eta^2}{1 + (k-2)\eta} \quad (1), \quad \eta \leq \frac{\varepsilon_{cu1}}{\varepsilon_c}, \quad \text{where}$$

parameters $\eta = \varepsilon_c / \varepsilon_{c1}$ and $k = 1.05 \cdot E_{cm} \cdot \varepsilon_{c1} / f_{cm}$ are also adopted according to Eurocode 2 [12]. Strain values $\varepsilon_{c1} = 2.2 \cdot 10^{-3}$ and $\varepsilon_{cu1} = 3.5 \cdot 10^{-3}$ are adopted from Table 3.1 from Eurocode 2 [12]. The used stress-strain curve recommended by Eurocode 2 [12] for strains $\varepsilon_c > \varepsilon_{cu1}$ is not defined. However, due to high stresses that may occur in concrete and that are larger than ε_{cu1} , there is a need for definition of descending branch. In this paper, descending branch recommended by Pavlović [11] is used:

$$\sigma_c = f_{cm} \cdot \left[\frac{1}{\beta} - \frac{\sin(\mu^{\alpha_{tD}} \cdot \alpha_{tE} \cdot \frac{\pi}{2})}{\beta \cdot \sin(\alpha_{tE} \cdot \frac{\pi}{2})} + \frac{\mu}{\alpha} \right] \quad (2)$$

In equation above, $\beta = f_{cm} / f_{cu1}$ and $\mu = (\varepsilon_c - \varepsilon_{cuD}) / (\varepsilon_{cuE} - \varepsilon_{cuD})$ represents relative coordinate between points D and E in Figure 9. In point D strain in concrete is $\varepsilon_{cuD} = \varepsilon_{cu1}$ and stress is calculated according to Equation (1) from Eurocode 2 [12]: $f_{cuD} = f_{cu1} = \sigma_c(\varepsilon_{cu1})$. The end of descending branch and the curve is defined by point E. Stress that corresponds to strain $\varepsilon_{cuE} = 0.03$ is $f_{cuE} = f_{cm} / \alpha$. Values of parameters α , α_{tD} , α_{tE} are usually determined in process of calibration of numerical model against experimental results. Since no experimental tests have been carried out for this work, values are adopted based on the data available in the literature [11].

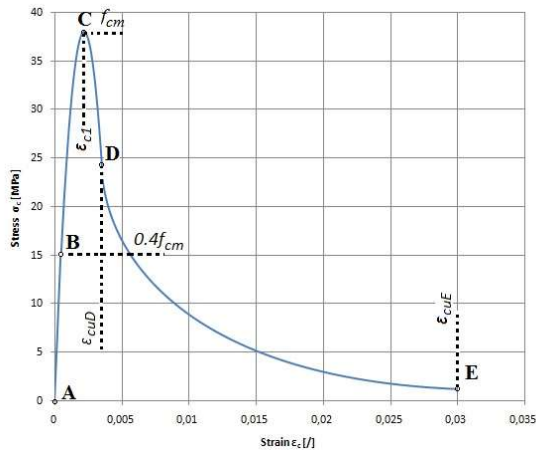


Figure 9. Stress-strain diagram for concrete C30/37 in compression

Strains $\varepsilon_{c,in}$ and stresses σ_c calculated according to Equations (1) and (2), depending on the total strain, are used as input data necessary to define plastic behaviour of concrete in compression in Abaqus [7]. Strains $\varepsilon_{c,in}$ are actually inelastic

strains that are calculated as:

$$\varepsilon_{c,in} = \varepsilon_c - \frac{\sigma_c}{E_{cm}} \quad (3).$$

The second input data is related to damage under compressive stresses. *Concrete damage parameter* (d_c) controls the damage level, and it is calculated as:

$$d_c = 1 - e^{-a_c \varepsilon_{c,in}} \quad (4)$$

In equation (4) $\varepsilon_{c,in}$ is strain and a_c is a parameter that can be changed in a calibration process. In this paper $a_c = 160$.

The similar concept is used for definition of concrete in tension in inelastic range. The curves are defined by stress and displacement values. Concrete is expected to behave linearly up to the value of its tensile strength $f_{ctm} = 2.9$ MPa. After this point, cracks occur in concrete and tensile stress depends on the crack width, as defined by Hordijk [13]:

$$\sigma_t(u) = f_{ctm} \cdot \left[\left[1 + \left(c_1 \frac{u}{u_c} \right)^3 \right] e^{-c_2 \frac{u}{u_c}} - \frac{u}{u_c} (1 + c_1^3) e^{-c_2} \right] \quad (5)$$

In Equation (5), tensile compressive strength is f_{ctm} and $c_1 = 3$ and $c_2 = 6.93$. Crack width is denoted by u , and u_c is critical crack width that corresponds to complete crack opening or point at which $\sigma_t = 0$. Recommendation for calculation of u_c is given by Hordijk [13]:

$$u_c = 5.14 \cdot G_F / f_{ctm} \quad (6),$$

where G_F is a fracture energy. In this study, fracture energy of concrete G_F is calculated according to recommendations of CEB-FIP Model Code 2010 [14]:

$$G_F = G_{F0} \cdot (f_{cm} / f_{ck0})^{0.7}; \quad f_{ck0} = 10 \text{ MPa} \quad (7)$$

The input data that is entered in Abaqus [7] and that is required to define behaviour of concrete in tension in inelastic range are crack width u and corresponding stress σ_t .

The second input data is related to damage under tensile stresses. Tensile damage is controlled by *Tensile damage parameter* (d_t) that is calculated as:

$$d_t = 1 - e^{-a_t \varepsilon_{t,ck}} \quad (8)$$

In this study parameter $a_t = 500$ and strain $\varepsilon_{t,ck}$ represents inelastic strain in tension. Strain $\varepsilon_{t,ck}$ is calculated as:

$$\varepsilon_{t,ck} = \varepsilon_t - \frac{\sigma_t}{E_{cm}} \quad (9)$$

Total strain ε_t is calculated according to recommendation from Almansa et al. [15]:

$$\varepsilon_t = \varepsilon_{el} + u / l_{eq} \quad (10),$$

where characteristic crack length is $l_{eq} = 50$ mm.

7. ANALYSIS

7.1 Results of numerical study

Described model is used for detailed analysis of stresses in all elements of composite connection under loading defined in Section 6.2. Firstly, response of steel elements (beams and column) is observed (Figure 10). Under the applied level of loading these elements mostly remain in elastic range. However, on contact of compressed beam flange and column, steel of beam flange and column web starts to yield (left joint side). In addition to this, as a result of compression of concrete slab on steel column, yielding of column web takes part too (right joint side).

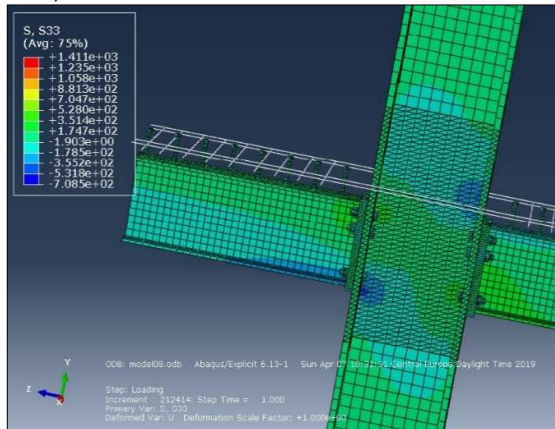


Figure 10. Stresses in steel elements under applied loading [MPa]

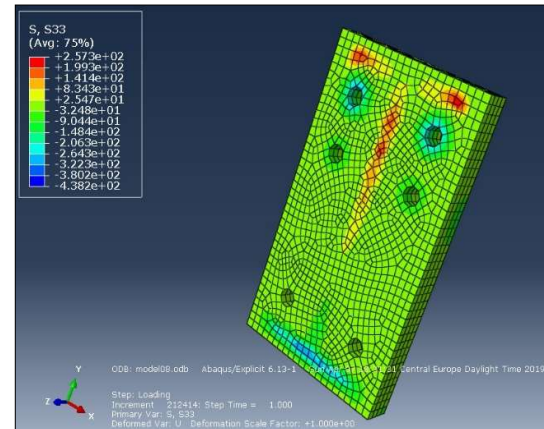


Figure 11. Stresses in steel plate under applied loading [MPa]

	σ [MPa]
Reinforcement	395.8
	340.9
	385.5
	323.0
First (upper) row of bolts	790.9
	800.1
Second (lower) row of bolts	137.0
	136.1

Table 3. Tensile stress in components of composite connection

Stresses in steel plate are shown in Figure 11. Steel yielding occurs in part subjected to tensile

stresses where a formation of T-element can be noticed. Furthermore, Figure 12 shows stresses in bolts. If stresses in the upper and lower row of bolts in tension are compared, it can be concluded that the first (upper) row of bolts takes part in transfer of tensile force more significantly than the lower row of bolts. The largest values of stresses in bolts are recorded in their contacts with nuts. In Table 3 average stress values measured in reinforcement, first and second row of bolts are summarized. These results indicate that the reinforcement is more activated than the second row of bolts.

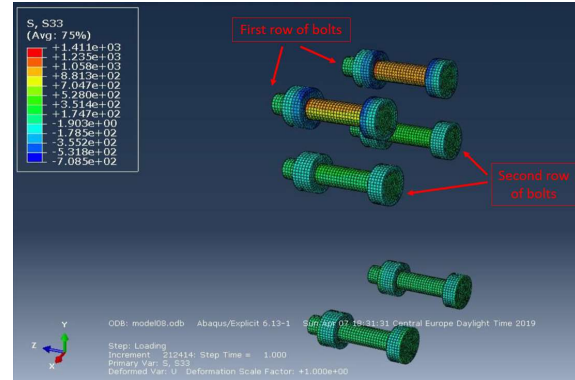


Figure 12. Stresses in bolts under applied loading [MPa]

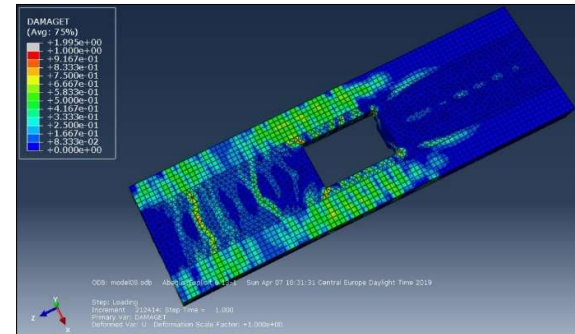


Figure 13. Distribution of cracks in concrete slab

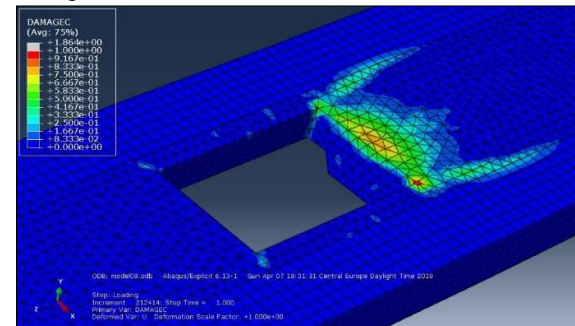


Figure 14. Compression damage in concrete slab

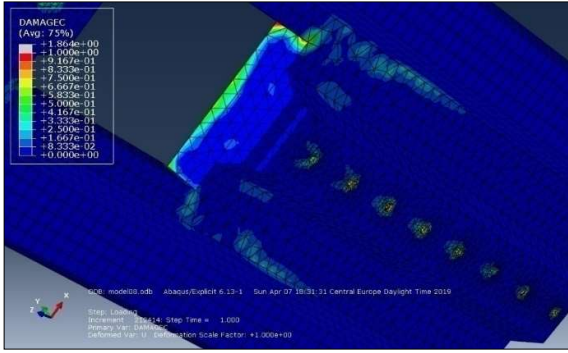


Figure 15. Compression damage in concrete slab due to local effect of shear stud connectors

Application of *Concrete damage plasticity* (CDP) model offers a possibility to detect cracks in concrete that occur due to tensile stresses, as well as damage in concrete due to compression stresses. The cracks distribution in concrete slab is presented in Figure 13. In the zone near beam – column joint cracks are more pronounced and tensile forces are transferred by reinforcement. Furthermore, compression damage to concrete slab can be observed close to contact of concrete slab and column (Figure 14), as well as around shear stud connectors due to local compressive stresses (Figure 15).

7.2 Mesh sensitivity

In order to check the reliability of results presented above, mesh sensitivity study is carried out. Two more models are built (Model01b and Model01c). Denser mesh is adopted on steel plate and column flange. In Model01 mesh size on steel plate and column flange is 10 mm and 20 mm, respectively. In Model01b, mesh size of 10 mm is kept on steel plate, but on column flange mesh size is reduced from 20 mm to 10 mm. In Model 01c, mesh size on both elements is reduced to 5 mm. Distribution of stresses remains unchanged and in Table 4 stresses measured in bolts bodies and reinforcement bars in three considered models are summarized.

	σ [MPa]		
	Model01	Model01b	Model01c
Reinforcement	395.8	398.6	404.1
	340.9	328.1	336.8
	385.5	381.9	386.9
	323.0	336.6	332.9
First (upper) row of bolts	790.9	794.4	778.3
	800.1	799.0	790.5
Second (lower) row of bolts	137.0	137.2	135.2
	136.1	139.2	136.1

Table 4. Stresses measured in reinforcement bars and bolts bodies for three models with different mesh size

7.3 Parametric study

The real effective width of concrete slab is investigated in parametric study. In addition to described model (Model 01) that has in total four reinforcement bars placed in effective slab width

$b_{eff,1} = 750$ mm, adopted according to Eurocode 4 [1], two more models are built. The second model (Model 02) has four more reinforcement bars than Model 01. They are placed in effective slab width $b_{eff,2} = 1100$ mm. This model is considered as the one corresponding to recommendations of Eurocode 8 [2]. The third model (Model 03) has eight reinforcement bars more than Model 01 placed in effective slab width $b_{eff,3} = 1500$ mm. It was included in the parametric study in order to investigate the stresses in the reinforcement, as well as the total tensile force that can be transferred by reinforcement, if the effective width is further widened. The same mesh density is used in additional two models (Model 02, Model 03) as in the original model (Model 01), as results of mesh sensitivity study confirmed the reliability of adopted mesh size. The same load is applied to all three models and average stresses in reinforcement bars are measured (Table 5). Additionally, in Figure 16 diagram which shows these stress values in reinforcement bars is presented. Reinforcement bars are defined based on their distance from the column axis. Diagram clearly shows decrease of stresses in reinforcement bars with increase of number of reinforcement bars (increase of effective slab width).

Distance from bar to column axis [mm]	Model01	Model02	Model03
	S_{11} [MPa]		
-700			85.1
-600			125.0
-500		196.1	137.7
-400		202.6	149.6
-300	340.9	236.4	170.1
-200	395.8	298.6	234.5
200	385.5	293.0	241.2
300	323.0	220.6	185.7
400		165.0	167.8
500		142.2	137.6
600			108.6
700			98.7

Table 5. Normal stresses in reinforcement bars

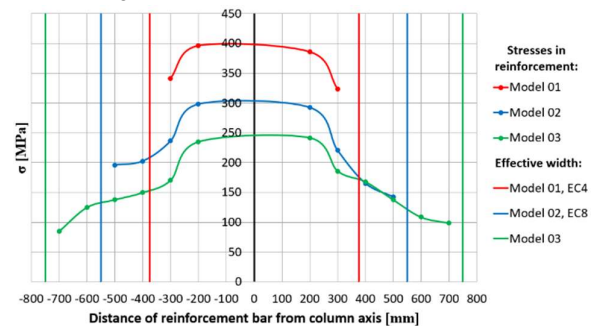


Figure 16. Stress in reinforcement bars as a function of bar location and model

If two bars from Model 01 that are closest to the column axis (-200 mm; +200 mm) are observed,

stresses in them decrease for about 25 % due to adding of four more bars (Model 02). By adding eight new bars stresses in these two bars decrease for about 40 % (Model 03). Stresses in bars in Model 01 that are further from column axis (-300 mm; +300 mm) decrease for about 30 % due to adding of four new bars (Model 02), while due to adding of eight new bars these stresses decrease for about 46 % (Model 03). These changes in stresses in reinforcement bars are summarized in Table 6.

Stresses in bars in Model 02 that are located at -400 mm and -500 mm from column axis decrease for about 30 % due to additional four bars in Model 03, while stresses in bars that are located at +400 mm and +500 mm remain almost unchanged (Table 7).

Distance from bar to column axis [mm]	Difference in stresses [%] Model 01 vs 02	Difference in stresses [%] Model 01 vs 03
-300	30.6	50.1
-200	24.6	40.8
200	24.0	37.4
300	31.7	42.5

Table 6. Change of stresses in reinforcement bars due to adding of new reinforcement bars

Distance from bar to column axis [mm]	Difference in stresses [%] Model 02 vs 03
-400	26.2
-500	29.8
400	-1.7
500	3.3

Table 7. Change of stresses in reinforcement bars due to adding of new reinforcement bars

Table 8 shows the total tensile force that is transferred by reinforcement in effective slab width in each model. If effective slab width is increased from $b_{eff,1} = 750$ mm (Model 01, EC 4 [1]) to $b_{eff,2} = 1100$ mm (Model 02, EC8 [2]), eight bars are considered in design instead of four. This leads to increase of 17.6 % total tensile force transferred by reinforcement. In addition to this, the stresses in bars that are the most distant from the column axis are in average 43 % smaller than stresses in the bars closest to column axis in Model 02.

	Total tensile force [kN]
Model 01	163.4
Model 02	198.4
Model 03	208.3

Table 8. Total tensile force transferred by reinforcement in effective slab width in each model
 If effective slab width is further widened ($b_{eff,3} = 1500$ mm), in total twelve reinforcement bars can be taken into account in design (Model 03). In this case, reinforcement is able to transfer only 4.73 % larger total tensile force than in Model 02. Additionally, stresses in bars that are the most distant from the column axis are in average 61.4

% smaller than stresses in bars closest to column axis.

Results of conducted parametric study show that the effective slab width in Model 02 ($b_{eff,2}$) adopted according to Eurocode 8 [2] provides the most favourable results in terms of the total tensile force that can be transferred by the reinforcement and level of exploitation of the reinforcement bars. By increasing the number of bars from four (Model 01) to eight (Model 02) it is possible to transfer the larger total tensile force and stresses in the least loaded bars are about 43 % smaller than stresses in the most loaded bars. With further adding of reinforcement bars, and increase of effective slab width ($b_{eff,3}$) in Model 03, the tensile force remains almost unchanged in comparison to Model 02 (difference is less than 5 %) and stresses in the least loaded bars are 61.4 % smaller than stresses in the most loaded bars. It can be concluded that in the case of seismic loading application of proposal for calculation of the effective slab width given in Eurocode 8 [2] is justified. However, this should be further investigated on different beam – to – column connections.

8. CONCLUSION

In this paper behaviour of composite steel – concrete beam – to – column connections with steel plate and bolts in tension is firstly theoretically explained using the component approach. Furthermore, one typical composite connection located in a moment-resisting frame of a 9-story commercial building designed according to Eurocode 4 [1] is chosen for a detailed analysis. Numerical model of composite connection is built in a software package Abaqus [7]. In order to simulate case of seismic loading, maximum bending moment and maximum shear force obtained from linear time-history analysis carried out on a spatial building model in SAP 2000 [6] are applied to the finite element model of composite connection in Abaqus [7]. Behaviour of composite connection is studied in detail, analyzing the stresses in steel and concrete elements, as well as crack propagation in concrete elements. Finally, parametric study is carried out in order to investigate justification of the adoption of wider effective slab width in case of seismic loading. Results of parametric study show that the total tensile force that is transferred by reinforcement bars expectedly increases with increase of reinforcement bars (and effective slab width), but the stresses in the more distant bars decrease, meaning that these reinforcement bars are not fully exploited. In this sense, it is concluded that for the considered beam – to – column composite connection effective width ($b_{eff,2}$, Model 02) adopted according to recommendations from Eurocode 8 [2] gives the

most favourable results, as four more reinforcement bars than in Model 01 ($b_{eff,1}$, EC4) transfer larger total tensile force, leaving the ratio of stresses in the most and least loaded bar in the reasonable range. The further increase of the effective width, as in Model 03, leads to negligible increase of the total tensile force transferred by reinforcement bars and to significantly smaller exploitation of reinforcement bars. Based on the results of the studied composite beam – to – column connection, it can be concluded that for seismic loading recommendations for calculation of effective slab width given in Eurocode 8 [2] should be used. Nevertheless, further studies with a more detailed focus on the failure modes and connection capacities of the beam – to – column connections with various geometries and material properties are required for a general conclusion, as there are many parameters that affect seismic performance of composite connections.

Aleksa Milijaš is the Chair of Structural Analysis and Dynamics at RWTH Aachen University, Aachen, Germany.

E-mail: milijas@lbb.rwth-aachen.de

For more details on semantics of your paper, see the following:

V. Milutinovic, "The Best Method for Presentation of Research Results," IEEE TCCA Newsletter, September 1997, pp. 1-6.

<http://www.computer.org/tab/tcca/news/sept96/sept96.htm>

REFERENCES

- [1] EN 1994-1-1(2004): Eurocode 4: Design of composite steel and concrete structures. Part 1-1: General rules and rules for buildings. CEN, Brussels, Belgium.
- [2] EN 1998-1 (2004). Eurocode 8: Design of structures for earthquake resistance. Part 1: General rules, seismic actions and rules for buildings (EN 1998-1). CEN, Brussels, Belgium.
- [3] EN 1991-1(2002): Eurocode 1 – Actions of structures. Part 1: General actions – Densities, self-weight, imposed loads on buildings. CEN, Brussels, Belgium.
- [4] EN 1993-1-1(2005). Eurocode 3: Design of steel structures – Part 1-1: General rules and rules for buildings. CEN, Brussels, Belgium.
- [5] Milijaš A., Analiza ponašanja spregnutih veza u objektima visokogradnje pri dejstvu zemljotresa“. Master thesis, Faculty of Civil Engineering, University of Belgrade, Serbia, 2019 (In Serbian)
- [6] Computer & Structures.SAP2000, Advanced 14.0 Structural AnalysisProgram – Manual. Computer and Structures, Inc, Berkeley, California,USA, 2010
- [7] Abaqus (2013). User Manual. Version 6.13. Providence, RI, USA: DS SIMULIA Corp.
- [8] Kupfer, H., Hilsdorf, H. K., and Rusch, Behavior of concrete under biaxial stresses. In Journal Proceedings (Vol. 66, No. 8, pp. 656-666), 1969
- [9] Lee, J., and Fenves, G. L., Plastic-damage model for cyclic loading of concrete structures. Journal of engineering mechanics, 124(8), 892-900, 1998
- [10] Jankowiak, T., and Lodygowski, T., Identification of parameters of concrete damage plasticity constitutive model. Foundations of civil and environmental engineering, 6(1), 53-69, 2005
- [11] Pavlović, M., Resistance of bolted shear connectors in prefabricated steel-concrete composite decks. University of Belgrade, 2013
- [12] EN 1992-1-1(2004). Eurocode 2: Design of concrete structures - Part 1-1: General rules and rules for buildings. CEN, Brussels, Belgium.
- [13] Hordijk, D.A., Tensile and tensile fatigue behavior of concrete; experiments, modeling and analyses. In, Heron 37(1): 3-79, 1992
- [14] CEB-FIP (2010). CEB-FIP Model Code 2010. Model code for concrete structures. International Federation for Structural Concrete (fib).
- [15] Lopez-Almansa, F., Alfarah, B., & Oller, S., Numerical simulation of RC frame testing with damaged plasticity model. Comparison with simplified models. In *Second European conference on Earthquake Engineering and Seismology, Istanbul, Turkey*, 2014